Differences in Active Site Gorge Dimensions of Cholinesterases Revealed by Binding of Inhibitors to Human Butyrylcholinesterase†

Ashima Saxena,*,‡ Ann M. G. Redman,‡ Xuliang Jiang,§ Oksana Lockridge,|| and B. P. Doctor‡

Division of Biochemistry, Walter Reed Army Institute of Research, Washington, D.C. 20307, The Integrated Program, College of Physicians and Surgeons of Columbia University, New York, New York 10032, and Eppley Cancer Institute, University of Nebraska Medical Center, Omaha, Nebraska 68198

Received June 13, 1997; Revised Manuscript Received August 22, 1997⊗

ABSTRACT: Amino acid sequence alignments of cholinesterases revealed that 6 of 14 aromatic amino acid residues lining the active center gorge of acetylcholinesterase are replaced by aliphatic amino acid residues in butyrylcholinesterase. The Y337(*F330*) in mammalian acetylcholinesterase, which is replaced by A328 in human butyrylcholinesterase, is implicated in the binding of ligands such as huperzine A, edrophonium, and acridines and one end of bisquaternary compounds such as BW284C51 and decamethonium. Y337 may sterically hinder the binding of phenothiazines such as ethopropazine, which contains a bulky exocyclic substitution. Inhibition studies of (−)-huperzine A with human butyrylcholinesterase mutants, where A328 (K_I = 194.6 μM) was modified to either F (K_I = 0.6 μM, as in *Torpedo* acetylcholinesterase) or Y (K_I = 0.032 μM, as in mammalian acetylcholinesterase), confirmed previous observations made with acetylcholinesterase mutants that this residue is important for binding huperzine A. Inhibition studies of ethopropazine with butyrylcholinesterase mutants, where A328 (K_I = 0.18 μM) was modified to either F (K_I = 0.82 μM) or Y (K_I = 0.28 μM), suggested that A328 was not solely responsible for the selectivity of ethopropazine. Volume calculations for the active site gorge showed that the poor inhibitory activity of ethopropazine toward acetylcholinesterase was due to the smaller dimension of the active site gorge which was unable to accommodate the bulky inhibitor molecule. The volume of the butyrylcholinesterase active site gorge is ∼200 Å^3 larger than that of the acetylcholinesterase gorge, which allows the accommodation of ethopropazine in two different orientations as demonstrated by rigid-body refinement and molecular dynamics calculations.

In vertebrates, two types of cholinesterases (ChEs)[1] can be distinguished on the basis of their substrate specificity and sensitivity to various inhibitors (*1*, *2*). Acetylcholinesterase (AChE, EC 3.1.1.7), which is predominantly present in the muscle and nervous system, causes the termination of impulse transmission by rapid hydrolysis of acetylcholine (*3*). Butyrylcholinesterase (BChE, EC 3.1.1.8) is primarily synthesized in the liver and secreted into the plasma. Although AChEs are most efficient at hydrolyzing acetylcholine, BChEs exhibit less specificity toward their substrate and efficiently hydrolyze butyryl- and acetylcholine as well as benzoylcholine. The two enzymes also differ in their sensitivity to inhibitors; BW284C51 and huperzine A specifically inhibit AChE, and ethopropazine and iso-OMPA specifically inhibit BChE. Molecular cloning and protein sequencing studies have revealed 70−72% sequence similarity and 51−54% sequence identity between mammalian AChE and BChE (*4*, *5*). The marked homology in the amino acid sequence of AChE and BChE has enabled the development of models of mammalian AChE and BChE based on the three-dimensional structure of *Torpedo* AChE (*6*).

Using site-specific mutagenesis and molecular modeling studies, three distinct domains of the ChE molecule have been shown to contribute to the binding of ChE inhibitors (*7*). Within each domain there is a cluster of aromatic amino acid residues that is responsible for substrate and inhibitor specificity (*8*). The acyl pocket of mammalian AChE is defined by two F residues at positions 295(*288*)[2] and 297(*290*), which are responsible for markedly reducing BTC hydrolysis and enhancing ATC hydrolysis by forming a clamp around the methyl moiety of the acyl group and restricting its degree of freedom (*7*). Replacement of either of these residues with aliphatic amino acid residues, as in BChEs, results in increased hydrolysis of BTC by the mutant enzyme and increased sensitivity to the bulky BChE-specific organophosphate inhibitor iso-OMPA (*7*, *8*, *10*, *11*). This observation is also supported by a naturally occurring mutation in *Drosophila* AChE that contains a single F at position 368(*290*). Replacement of this F by Y confers enzyme resistance to certain organophosphates (*12*). A second cluster of aromatic amino acid residues in mammalian AChEs, Y72(*70*), Y124(*121*), and W286(*279*), is located near

† This work was supported in part by United States Army Medical Research and Materiel Command Grant DAMD17-94-J-4005 (to O.L.).

* Corresponding author.
‡ Walter Reed Army Institute of Research.
§ College of Physicians and Surgeons of Columbia University.
|| University of Nebraska Medical Center.

⊗ Abstract published in *Advance ACS Abstracts,* October 15, 1997.

[1] Abbreviations: ChE, cholinesterase; AChE, acetylcholinesterase; BChE, butyrylcholinesterase; ATC, acetylthiocholine; BTC, butyrylthiocholine; DTNB, 5,5′-dithiobis(2-nitrobenzoic acid); MEPQ, 7-[(methylmethoxyphosphinyl)oxy]-1-methylquinolinium; BW284C51, 1,5-bis-[*p*-(allyl-*N*,*N*-dimethylammonio)phenyl]pentan-3-one; iso-OMPA, tetraisopropylpyrophosphoramide; ethopropazine, 10-[2-(diethylamino)-propyl]phenothiazine; tacrine, 9-amino-1,2,3,4-tetrahydroacridine; edrophonium, ethyl(*m*-hydroxyphenyl)dimethylammonium chloride; propidium, 3,8-diamino-5-[3′-(diethylmethylammonio)propyl]-6-phenylphenanthridinium iodide; TMTFA, *m*-(*N*,*N*,*N*-trimethylammonio)trifluoroacetophenone.

[2] The dual numbering system gives the residue number in the species designated followed by the corresponding residue in *Torpedo* AChE (*9*).

S0006-2960(97)01425-6 CCC: $14.00

the lip of the gorge and has been designated as part of the "peripheral" anionic site. Mutation of W286 to A, as in BChE, results in a loss of sensitivity of the mutant enzyme to ligands like BW284C51 and propidium (*10*, *13*). The two neighboring Y residues at positions 72(*70*) and 124(*121*) also contribute to the stabilization of peripheral site inhibitor complexes (*8*). Two aromatic amino acid residues, W86(*84*) and Y337(*330*), are part of the choline binding site (*6*). The role of W86(*84*), which is conserved in all ChEs, in the orientation and stabilization of the quaternary ammonium group of the substrate, has been demonstrated by chemical labeling studies (*14*, *15*), by crystallographic data (*6*, *16*), and by site-directed mutagenesis studies (*11*). The Y at position 337 in mammalian AChE is replaced by F in *Torpedo* AChE and A in human BChE. This residue appears to stabilize the binding of ligands such as huperzine A, edrophonium, and acridines and one end of bisquaternary compounds such as BW284C51 and decamethonium (*8*, *10*, *11*, *13*, *17*, *18*). This residue destabilizes the binding of phenothiazines such as ethopropazine, which contains a bulky exocyclic substitution. Structure−activity relationships show that this is a consequence of steric hindrance between the diethylamino-2-isopropyl moiety with the aromatic side chain of Y337(*330*) in the mammalian enzyme (*8*).

In this paper we examined the inhibition of human BChE mutants by ethopropazine and other inhibitors of ChEs, where A328(*F330*) was modified to F, as in *Torpedo* AChE, or Y, as in mammalian AChE. In delineating the role of this residue in the binding of various inhibitors to ChEs, we found that for (−)-huperzine A, edrophonium, tacrine, and BW284C51 interpretations made from studies with AChE mutants correlated with those made from studies with BChE mutants. On the other hand, with ethopropazine the results obtained with AChE mutants (*8*) could not be correlated with those obtained with BChE mutants. Using molecular modeling studies, it was demonstrated that the larger dimension of the BChE gorge could account for the higher potency of ethopropazine for BChE compared to AChE.

EXPERIMENTAL PROCEDURES

Materials for Inhibition Studies. Acetylthiocholine (ATC), butyrylthiocholine iodide (BTC), 5,5′-dithiobis(2-nitrobenzoic acid) (DTNB), ethyl(*m*-hydroxyphenyl)dimethylammonium chloride (edrophonium), 10-[2-(diethylamino)propyl]-phenothiazine (ethopropazine), 9-amino-1,2,3,4-tetrahydroacridine (tacrine), 3,8-diamino-5-[3′-(diethylmethylammonio)propyl]-6-phenylphenanthridinium iodide (propidium), decamethonium, and 1,5-bis[*p*-(allyl-*N*,*N*-dimethylammonio)-phenyl]pentan-3-one (BW284C51) were obtained from Sigma Chemical Co. (St. Louis, MO). (−)-Huperzine A isolated from *Huperzia serrata* was purchased from Dr. Liu Jia Sen (Alberta, Canada). The structures of the inhibitors used in this study are shown in Figure 1. Electrophoretically pure AChE from FBS was purified as described (*19*), and AChE from *Torpedo californica* was provided by Professor I. Silman (Weizmann Institute of Science, Rehovot, Israel). Purified BChE from human serum and 7-[(methylmethoxyphosphinyl)oxy]-1-methylquinolinium (MEPQ) were provided by Dr. Yacov Ashani (Israel Institute for Biological Research, Ness-Ziona, Israel). One milligram of pure native AChE or BChE contained approximately 14 and 12 nmol of active sites, respectively.

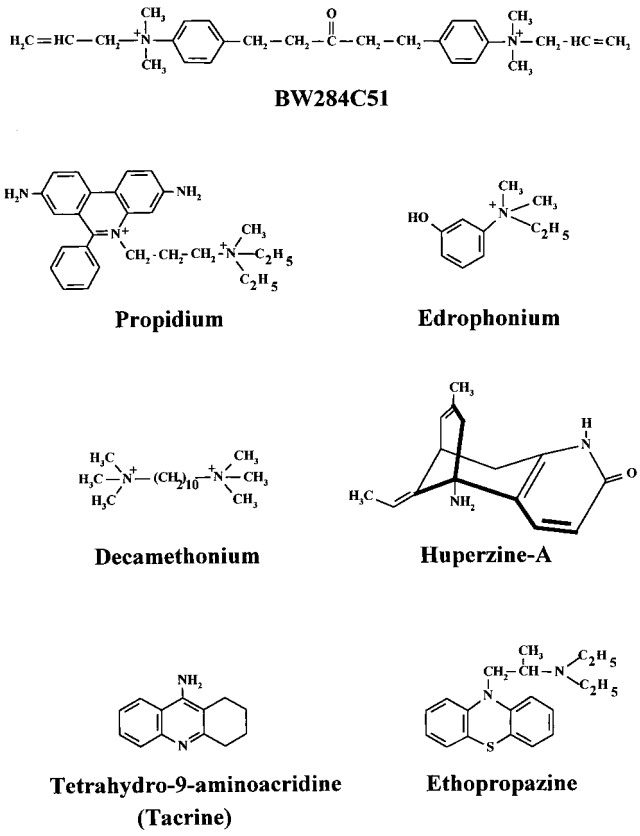

FIGURE 1: Structures of cholinesterase inhibitors.

Materials for Molecular Modeling Studies. The atomic coordinates of *T. californica* AChE and its complexes with inhibitors and the mouse AChE−fasciculin 2 complex were obtained from the Protein Data Bank, Chemistry Department, Brookhaven National Laboratory, Upton, NY. The coordinates for human BChE were from a model (*10*) and for ethopropazine from its X-ray crystal structure (*20*).

Mutagenesis and Expression of Human Butyrylcholinesterase. The cDNA of human BChE (*21*) was modified to give the optimal ATG start site context GCCACCATGG for the ATG of the 28 amino acid leader sequence. Site-directed mutagenesis was performed with the polymerase chain reaction (PCR) and Pfu DNA polymerase (Stratagene, La Jolla, CA) in a protocol similar to that of Chen and Przybyla (*22*). The codon for A328 (GCT) was replaced with the codon for F (TTT) or Y (TAT). The 1.8 kb PCR fragment was purified with the QIAquick-spin PCR purification kit (Qiagen, Chatsworth, CA) to remove Pfu polymerase, then digested with *Hin*dIII and *Apa*I, and purified a second time on a QIAquick-spin column to remove *Hin*dIII and *Apa*I enzymes. The 1.8 kb fragment was ligated into the expression plasmid pGS (Dr. Tyler White, Scios Nova, Mountain View, CA). The cloned BChE was completely resequenced to ensure the absence of unwanted mutations. Oligonucleotide synthesis and DNA sequencing were performed by the University of Nebraska Molecular Biology Core Facility directed by Charles Mountjoy. Plasmid DNA, purified with the Qiagen plasmid kit (Qiagen, Chatsworth, CA) was transfected into CHO K1 cells (ATCC No. CCL 61, Rockville, MD) by calcium phosphate coprecipitation. The pGS plasmid is similar to pRc/CMV (Invitrogen, San Diego, CA) but has rat glutamine synthase in place of the neomycin resistance gene. Two days after transfection selection was

Scheme 1

$$\begin{array}{ccccc} E + S & \rightleftarrows & ES & \xrightarrow{k_{cat}} & E + P \\ + & & + & & \\ S & & S & & \\ K_{ss}\downarrow\uparrow & & K_{ss}\downarrow\uparrow & & \\ SE + S & \rightleftarrows & SES & \xrightarrow{bk_{cat}} & SE + P \end{array}$$

Scheme 2

$$\begin{array}{ccccc} E + S & \rightleftarrows & ES & \xrightarrow{k_{cat}} & E + P \\ + & & + & & \\ I & & I & & \\ K_I\downarrow\uparrow & & \downarrow\uparrow \alpha K_I & & \\ EI + S & \rightleftarrows & ESI & & \end{array}$$

begun with glutamine-free, serum-free medium (Ultraculture 12-725B, BioWhittaker, Walkersville, MD) containing 50 μM methionine sulfoximine (Sigma, St. Louis, MO). Resistant colonies appeared 3−5 weeks later. Colonies were picked with a sterile cotton-tipped stick for transfer to 24-well cluster plates. Clones with the highest BChE activity were expanded into T150 flasks. Secreted BChE was collected into serum-free medium, filtered through a 0.45 μm filter to remove particulates, and concentrated in an Amicon stirred cell with a PM10 membrane (Amicon, Beverly, MA). The activity of the concentrated enzyme was 10−60 units/mL measured, as described below (*23*).

Measurement of Cholinesterase Activity and Inhibition. AChE and BChE activities were measured in 50 mM sodium phosphate buffer, pH 8.0, at 22 °C as described (*23*) using ATC and BTC as substrates, respectively. Active sites were quantitated by titration with a high-affinity phosphorylating agent, MEPQ, to ascertain the minimal concentration required for the complete inhibition of enzyme activity (*24*). Inhibition of enzyme activity was measured in 50 mM sodium phosphate buffer, pH 8.0, over a substrate concentration range of 0.01−0.25 mM and using at least three inhibitor concentrations to determine the components of competitive and uncompetitive inhibition. Inhibition studies with propidium were carried out in 5 mM sodium phosphate buffer, pH 8.0.

Analysis of Catalytic Parameters. The catalytic parameters of wild-type and mutant BChEs were compared by measuring catalysis as a function of BTC concentration. For BChE, the interaction of substrate (S) with enzyme (E) can be described more appropriately as shown in Scheme 1, where the substrate binds to two discrete sites on the enzyme molecule forming two binary complexes, ES and SE (*8*). In this scheme, K_{ss} represents the binding of a substrate molecule to the binary enzyme−substrate complexes and b reflects the efficiency of hydrolysis of the ternary complex, SES, compared to the binary complex, ES (*25*). Scheme 1 is described by the equation:

$$v = \left(\frac{1 + b[S]/K_{ss}}{1 + [S]/K_{ss}}\right)\left(\frac{V_{max}}{1 + K_m/[S]}\right)$$

Analysis of Inhibition Data. The interaction of an inhibitor (I) with an enzyme (E) can be described by Scheme 2. In this scheme, ES is the enzyme−substrate complex and P is the product. K_I and αK_I are the inhibition constants reflecting the interaction of inhibitor with the free enzyme and the enzyme−substrate complex, respectively. A plot of reciprocal velocities versus reciprocal substrate concentrations (Lineweaver−Burk plot) at a series of inhibitor concentrations yields a family of slopes and y intercepts. Replots of the slope and y-intercept values versus inhibitor concentrations were used for the determination of K_I and αK_I values, respectively.

Structural Comparisons and Volume Calculations of the Active Site Gorge. The X-ray crystal structures of AChE and its complexes with inhibitors were compared using LSQ utilities of program O (*26*). The calculations of the van der Waals volume for ethopropazine and of the probe-accessible volumes of the active site pockets for *Torpedo* AChE, human BChE, and their mutants were performed using VOIDOO (version 3.1) (*27*). The radius of the probe was 1.4 Å, and each calculation was refined for 10 cycles. The relative sizes of the active site gorges of AChE and BChE were calculated by placing a planar cover consisting of 126 carbon atoms at the entrance to the active site gorge. In all cases the covers were placed at identical positions around residues 71, 74, 276, 280, 285, and 335. Mutations were introduced using the MUTATE utilities of O (*26*), and all of the possible rotamers for each mutation as defined in the database of O were evaluated. The rotamer possessing the lowest energy as calculated by X-PLOR (*28*) was used for volume calculations.

Molecular Modeling. The binding of ethopropazine to AChE was modeled using Insight II (version 2.3.0, Biosym Technologies, San Diego, CA) and the X-ray crystal structures of *T. californica* AChE (*6*) and ethopropazine (*20*). The atomic structure of human BChE was a reconstructed model based on the structure of *T. californica* AChE (*10*). Molecular modeling was carried out in three sequential steps on a Silicon Graphics Indigo 2 workstation. First, the hydrogen atoms of ethopropazine, *Torpedo* AChE, and human BChE were built using the Builder module of the Insight II program with the dissociation state of ionizable groups set equivalent to the experimental condition of pH 8.0. The ethopropazine molecule was then manually docked into the active site gorge of AChE or BChE using the Docking module of Insight II. The orientations of the ethopropazine molecule in the active site gorge were extensively searched in the six-dimensional rotational and translational space. All the possible orientations were evaluated using the Docking module of Insight II, and the orientations with the lowest energy were defined as the ones for the complex structure.

In the second step, a rigid-body refinement of the low-energy orientations defined in the first step was carried out using X-PLOR (*28*). The topology and parameter files for the ethopropazine molecule were generated by the XPLO2D program in Kleywegt's XUTIL package (*29*). The partial charges for the atoms of the ethopropazine molecule used in the parameter file were calculated using the AMPAC module of Insight II.

The third step was a molecular dynamics routine in which the complexes from the previous modeling step were subjected to simulated annealing using X-PLOR (*28*). The complex structure was first heated to a temperature of 1000 K and then slowly cooled to 300 K, using intervals of 25 K, with each interval consisting of 50 steps and time step of 0.0005 ps. The dielectric constant used in the simulation was 4.0.

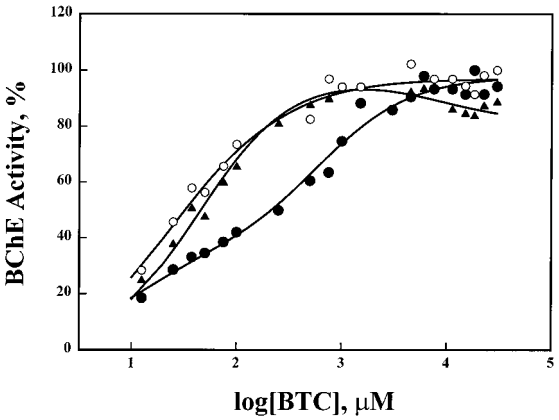

FIGURE 2: Substrate concentration dependence for butyrylthiocholine hydrolysis by recombinant human butyrylcholinesterases. Wild-type (●), A328F (○), and A328Y (▲) human BChE enzymes were assayed for activity using the Ellman assay (*23*) and BTC concentration range of 0.01−30 mM. Data were fit to eq 1, and values obtained for K_m, K_{ss}, and *b* are shown in Table 1.

RESULTS

Substrate Activation. Figure 2 shows the substrate concentration dependence for recombinant wild-type and mutant human BChE. The data were analyzed according to Scheme 1, which is described by eq 1. In this scheme, the binary ES complex as well as the ternary SES complex leads to the formation of product, although the rates of hydrolysis may differ (*8*). A mutation may affect the dissociation constant, K_{ss} or *b*, which is a factor describing the hydrolysis capacity of the SES complex. As shown in Table 1, for wild-type BChE, a *b* value of 2.7 suggested that the SES complex was more productive than the ES complex and resulted in substrate activation. However, mutating A328 to the corresponding aromatic amino acid residues found in *Torpedo* and mammalian AChEs, F and Y respectively, eliminated substrate activation, as demonstrated by the normalization of *b* values for the mutant enzymes. In both cases, since there was little or no substrate activation or inhibition, it was difficult to distinguish between a large K_{ss} and a value of *b* which approached 1.0 (Table 1). These results suggest that A328 conferred the property of apparent substrate activation to BChE.

To study the effect of these mutations on the catalytic parameters of the enzyme, we determined the k_{cat} of wild-type and mutant enzymes by comparing V_{max} to the number of active site serines, determined by direct titration with MEPQ. MEPQ retained a high apparent inhibitory activity for mutant BChEs and a linear concentration dependence, resulting in a stoichiometric titration. The k_{cat} values for wild-type, A328F, and A328Y BChE were nearly identical (Table 1). The k_{cat} value for wild-type BChE was 50 000 min^{-1}, which is similar to the value of 45 500 min^{-1} measured under identical assay conditions (Y. Ashani, personal communication) but higher than the value of 24 000 min^{-1} reported by Masson et al. (*30*). This difference in k_{cat} values is probably due to differences in assay conditions (ionic strength, pH, temperature, and buffer composition; Masson et al., measured activity in 0.1 M phosphate buffer, pH 7.0 at 25 °C).

Binding of Inhibitors to Cholinesterases. The role of A328(*F330*) in the binding of various inhibitors to BChE was examined by conducting inhibition studies with native ChEs as well as site-specific human BChE mutants.

(A) Huperzine A. The choline binding pocket of mammalian AChE is defined by W86(*84*) and Y337(*F330*). Molecular modeling and site-directed mutagenesis studies implicated these two residues in the binding of huperzine A to mammalian AChE (*17*, *18*). Y337 in mammalian AChE is replaced by A328 in BChE. To further support the fact that Y337 was responsible for the selectivity of huperzine A, we carried out corresponding studies with human BChE mutants. Inhibition studies of (−)-huperzine A with human BChE mutants (Table 2), where A328 (K_I = 194.6 μM) was modified to either F (*Torpedo* AChE; K_I = 0.6 μM) or Y (mammalian AChE; K_I = 0.032 μM), confirmed observations made with native ChEs (Table 3) and AChE mutants (*17*, *18*) that the binding was stronger when the amino acid at position 328(*330*) was aromatic (*31*). There is a remarkably close correlation in the $\Delta\Delta G$ of binding for (−)-huperzine A between Y337 mutations in AChE and A328 mutations in BChE (Table 4). These results further support the conclusion that Y337(*F330*) plays a major role in the binding of huperzine A to AChE.

(B) Edrophonium. Since Y337 was also involved in the binding of ligands such as edrophonium and acridines and one end of bisquaternary compounds such as BW284C51 and decamethonium, we compared the inhibition of native ChEs (Table 3) and human BChE A328 mutants (Table 2) by these inhibitors. Like huperzine A, inhibition studies of edrophonium with human BChE mutants, where A328 (K_I = 290.7 μM) was modified to either F (*Torpedo* AChE; K_I = 11.2 μM) or Y (mammalian AChE; K_I = 6.6 μM), confirmed observations made with native ChEs (Table 3) and AChE mutants (*8*, *13*) and implicate Y337 in the stabilization of the AChE−edrophonium complex.

(C) Tacrine. Inhibition of ChEs by tacrine revealed a 12-fold difference in K_I between human BChE and FBS AChE (Table 3). However, site-directed mutagenesis studies with mouse AChE Y337 mutants, where the K_I for tacrine decreased when Y was substituted for A as in human BChE, suggest that Y337(*F330*) was not involved in the stabilization of the AChE−tacrine complex (*8*). A similar result was obtained with human BChE mutants, as there were no significant differences in K_I for wild-type and the A328Y mutant BChE (Table 2).

(D) Decamethonium and BW284C51. The two bisquaternary inhibitors decamethonium and BW284C51 were also studied for their binding to native ChEs and A328 mutants. As shown in Table 3, decamethonium was a competitive inhibitor of human BChE as well as FBS AChE. There were no significant differences in K_I for recombinant wild-type and mutant BChEs (Table 2). However, for *Torpedo* AChE, decamethonium showed a mixed type of inhibition, suggesting that it was interacting with the free enzyme as well as the enzyme−substrate complex. For BW284C51, a 400-fold difference in K_I was observed between mammalian AChE and BChE (Table 3). Using human BChE A328 mutants, the higher K_I for BChE was correlated with an A substituted for Y in mammalian AChE (Table 2).

(E) Propidium. Propidium, a bisquaternary ligand, is a classical peripheral anionic site inhibitor of AChE that does not bind to the active site (*32*). Unlike decamethonium and BW284C51, where the quaternary nitrogens are maximally separated by a distance of 14 Å, the quaternary nitrogens in propidium are maximally separated by only 4.8 Å. Since the binding of peripheral anionic site ligands is enhanced in

Table 1: Kinetic Parameters for Recombinant Human Butyrylcholinesterase Mutants[a]

enzyme	K_m (μM)	K_{ss} (mM)	b	k_{cat} ($\times 10^5$/min)	k_{cat} ($\times 10^9$/min·M)
wild type	10.3 ± 7.0	0.63 ± 0.18	2.70 ± 0.5	0.5	4.9
A328F	22.5 ± 10.4		1.03 ± 0.5	0.3	1.4
A328Y	42.6 ± 4.0		0.81 ± 0.1	0.5	1.1

[a] Values for K_m, K_{ss}, and b were calculated using nonlinear fitting of data to eq 1. The values of K_{ss} are indeterminate when b approached a value of 1. k_{cat} was evaluated using MEPQ titrations. Enzyme assays were conducted in 50 mM sodium phosphate, pH 8.0 at 22 °C, as described (*23*).

Table 2: Dissociation Constants for the Inhibition of Recombinant Human Butyrylcholinesterases[a]

	enzyme					
	BChE, wild type		A328F		A328Y	
inhibitor	K_I (μM)	αK_I (μM)	K_I (μM)	αK_I (μM)	K_I (μM)	αK_I (μM)
(−)-huperzine A	194.6		0.6		0.032	
edrophonium	290.7	331.7	11.2	13.4	6.6	9.4
ethopropazine	0.2	0.12	0.8	0.5	0.24	0.34
tacrine	0.015	0.018	0.25	0.9	0.043	0.08
propidium	0.49		0.4		0.65	1.35
decamethonium	4.7		3.1		5.23	
BW284C51	5.4	57.7	0.5		0.18	

[a] Values for K_I (competitive inhibition constant) and αK_I (uncompetitive inhibition constant) were determined from analysis of slopes of $1/v$ versus $1/s$ at various inhibitor concentrations. Values are from at least three experiments. Standard errors are typically within 20% of the mean.

Table 3: Dissociation Constants for the Inhibition of Native Cholinesterases[a]

	enzyme					
	human BChE		*Torpedo* AChE		FBS AChE	
inhibitor	K_I (μM)	αK_I (μM)	K_I (μM)	αK_I (μM)	K_I (μM)	αK_I (μM)
(−)-huperzine A	75.6		0.25		0.006	
edrophonium	120.4		0.2		0.1	
ethopropazine	0.02	0.026	18.0	33.1	173.2	203.9
tacrine	0.007	0.053	0.01	0.01	0.083	0.09
propidium	0.4			0.03		0.36
decamethonium	2.2		0.6	0.83	4.1	
BW284C51	6.4	52.0	0.008	0.02	0.016	0.04

[a] Values for K_I (competitive inhibition constant) and αK_I (uncompetitive inhibition constant) were determined from analysis of slopes of $1/v$ versus $1/s$ at various inhibitor concentrations. Values are from at least three experiments. Standard errors are within 20% of the mean.

Table 4: Dissociation Constants and Free Energy Differences for the Inhibition of Mutant Cholinesterases by (−)-Huperzine A

	enzyme	K_I (μM)	$\Delta\Delta G$ (kcal)[a]
mouse AChE[b]	wild type	0.0085 ± 0.004	0.0
	Y337F	0.273 ± 0.01	2.1
	Y337A	8.2 ± 0.1	4.9
human BChE	wild type[c]	194.6 ± 10.1	0.0
	A328F[c]	0.60 ± 0.03	−3.4
	A328Y[c]	0.032 ± 0.005	−5.1

[a] Calculated according to the formula $\Delta\Delta G = RT \ln K'_I/K_I$, where K_I and K'_I are the dissociation constants for the mutant and wild-type ChE, respectively (*8*). [b] Values reported previously (*17*). [c] K_I values were determined from the slopes of $1/v$ versus $1/s$ plots using various concentrations of (−)-huperzine A.

low ionic strength solutions, inhibition studies with propidium were carried out in 5 mM sodium phosphate, pH 8.0. As shown in Table 3, propidium was an uncompetitive inhibitor of AChE and a competitive inhibitor of BChE. Competitive inhibition of human BChE by propidium suggests that it binds to the active site of BChE (*30*). Mutation of A328 to F or Y did not affect the binding of propidium to these mutants (Table 2), confirming earlier observations made with the corresponding human AChE mutants (*13*). A 12-fold difference in the affinity of propidium for *Torpedo* AChE and FBS AChE suggests that there are differences in the peripheral anionic site of these two enzymes.

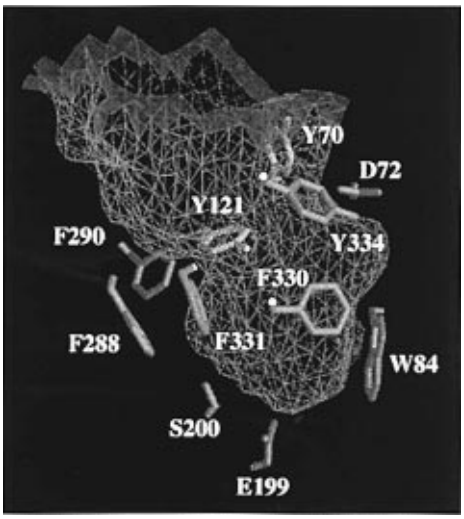

FIGURE 3: Volume calculations for the active site gorge of *Torpedo* acetylcholinesterase. The probe-accessible volume for the active site gorge of *Torpedo* AChE was calculated using VOIDOO (version 3.1) (*27*). The radius of the probe was 1.4 Å, and each calculation was refined for 10 cycles. The volume of the active site gorge was calculated by placing a planar cover consisting of 126 carbon atoms at the entrance of the active site gorge. The figure shows the placement of the cover (in blue) around residues 71, 74, 276, 280, 285, and 335 in *Torpedo* AChE and the region for which the volume was calculated. The figure was generated using GRASP (*42*).

(F) Ethopropazine. Inhibition studies with ethopropazine, a substituted phenothiazine, revealed a 9000-fold difference in K_I between human BChE and FBS AChE (Table 3). Using site-directed mutants of mouse AChE, it was demonstrated that Y337(*F330*) was responsible for sterically occluding the binding site for ethopropazine (*8*). However, our results with human BChE mutants A328Y and A328F (Table 2) did not show the dramatic differences in the binding of ethopropazine previously observed with mouse AChE mutants. These results suggest that the orientation of ethopropazine in the active site gorge of BChE may be different from that in the AChE gorge.

Structural Comparisons and Volume Calculations for the Active Site Gorges of Cholinesterases. The sizes of the active site gorges of *Torpedo* AChE and human BChE were compared quantitatively by calculating their probe-accessible volumes. Figure 3 shows the planar cover consisting of 126 carbon atoms that was placed at the entrance of the active site gorges so that they appeared as closed-up cavities in the calculation. The superimposed active site gorges of

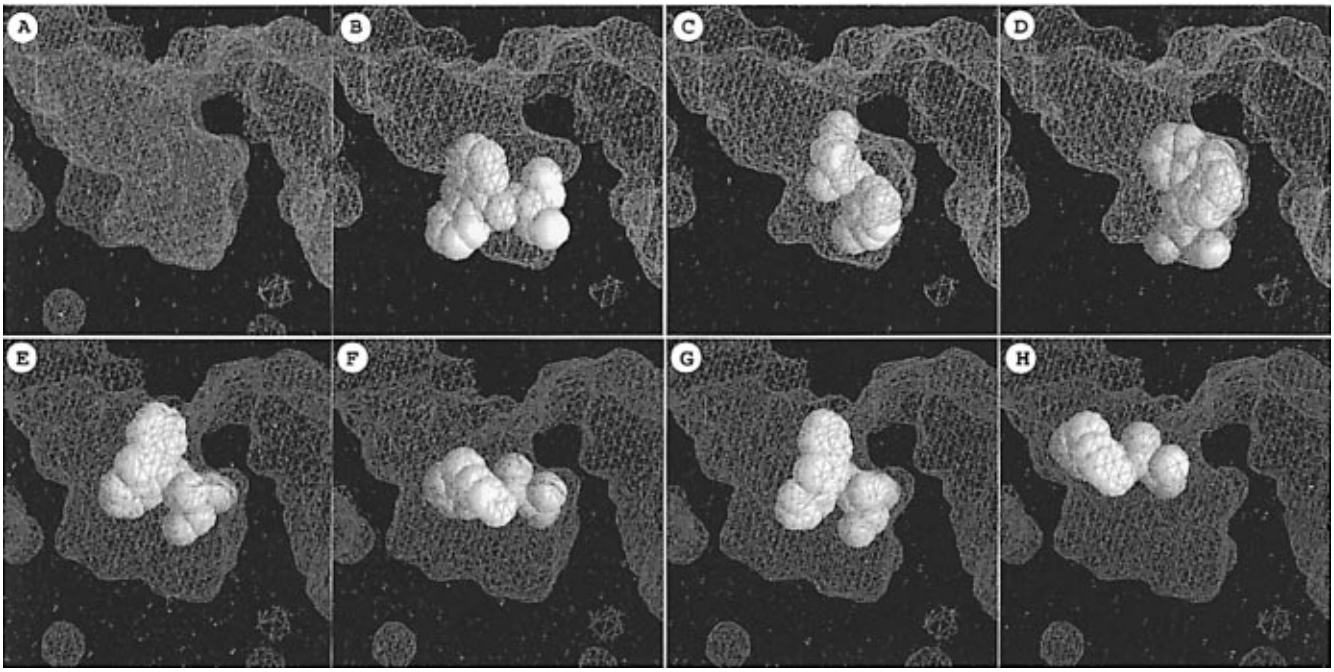

FIGURE 4: Rigid-body refinement structures of ethopropazine modeled into the active site gorge of cholinesterases. (A) The superimposed active site gorges of *Torpedo* AChE (magenta) and human BChE (green) are shown. The structure of *Torpedo* AChE was from its X-ray crystal structure (*6*), and that of human BChE was a model based on the structure of *Torpedo* AChE (*10*). The results of the rigid-body refinement calculations for the binding of ethopropazine to AChE and BChE are shown in panels B−H as follows: (B) *Torpedo* AChE, (C) F330A *Torpedo* AChE, first orientation, (D) F330A *Torpedo* AChE, second orientation, (E) human BChE, first orientation, (F) human BChE, second orientation, (G) A328(*330*)F human BChE, first orientation, and (H) A328(*330*)F human BChE, second orientation. The figure was generated using GRASP (*42*).

Table 5: Probe-Accessible Volumes of Active Site Gorges of Cholinesterases

	enzyme	volume of active site gorge (Å^3)	difference in volume[a] (Å^3)
Torpedo AChE	wild-type	302.31	
	F330A	337.68	35.37
	F339A	302.32	*b*
human BChE	wild type	501.91	199.60
	A330F[c]	410.35	108.04
	A330Y	405.55	103.24
ethopropazine[d]		317.6	

[a] Difference in volume of the active site gorge of enzyme compared to wild-type *Torpedo* AChE. [b] F339 of *Torpedo* AChE is located outside the cover used for calculating the volume of the active site gorge (Figure 3). Therefore, a mutation in this residue should not affect the volume of the gorge. [c] *Torpedo* numbering system. [d] van der Waals volume.

Table 6: Energy Difference (in kcal/mol) during Complex Formation[a]

	enzyme	orientation of ethopropazine	rigid-body refinement	molecular dynamics
Torpedo AChE	native		172.84	−9.06
	F330A[b]	1	−50.40	−58.03
		2	−19.40	−55.58
human BChE	native	1	−55.32	−41.96
		2	−59.07	−33.05
	A328(*330*)F	1	−79.93	−87.69
		2	−45.12	−116.59
	A328(*330*)Y	1	−87.75	−100.02
		2	−108.65	−74.30

[a] Negative and positive values correspond to complexes that are more and less stable, respectively, than separate enzyme and inhibitor. [b] *Torpedo* numbering system.

Torpedo AChE and human BChE are shown in Figure 4A, and the volumes of the active site gorges calculated for wild-type and mutant ChEs are shown in Table 5. The probe-accessible volume of the AChE active site gorge is 302.31 Å^3, which is less than the van der Waals volume of 317.6 Å^3 for ethopropazine. This result demonstrates that the poor inhibitory potency of ethopropazine toward AChE is due to the smaller dimension of the active site gorge which is unable to accommodate the bulky inhibitor molecule (Figure 4B). The mutation of F330 to A in *Torpedo* AChE increases the volume of the gorge to 337.68 Å^3 and allows the accommodation of ethopropazine (Figure 4C,D). The volume of the BChE active site gorge is ∼200 Å^3 larger than that of the AChE gorge, and this difference in the dimension of the active site gorge can account for better accommodation and differences in the binding of bulky substrate and inhibitor molecules to ChEs.

Molecular Modeling of Ethopropazine Binding to Cholinesterases. Due to the availability of the X-ray crystal structures of ethopropazine (*20*) and *Torpedo* AChE (*6*), and a model for human BChE (*10*), we attempted to model ChE−ethopropazine complexes to interpret our kinetic data. Ethopropazine was docked into the active sites of *Torpedo* AChE and human BChE and their mutants followed by rigid-body refinement calculations (Figure 4B−H). The changes in energy that the enzyme molecule undergoes upon complexation with ethopropazine for various ChE−ethopropazine complexes are shown in Table 6. These results confirm the conclusions made from volume calculations that the active site gorge of AChE is not large enough to accommodate ethopropazine (Figure 4B) while that of BChE can easily accommodate the inhibitor in two different orientations (Figure 4E,F). The F330 to A mutation in AChE dramatically removes the steric hindrance and allows the accommodation of ethopropazine (Figure 4C,D). In contrast, the

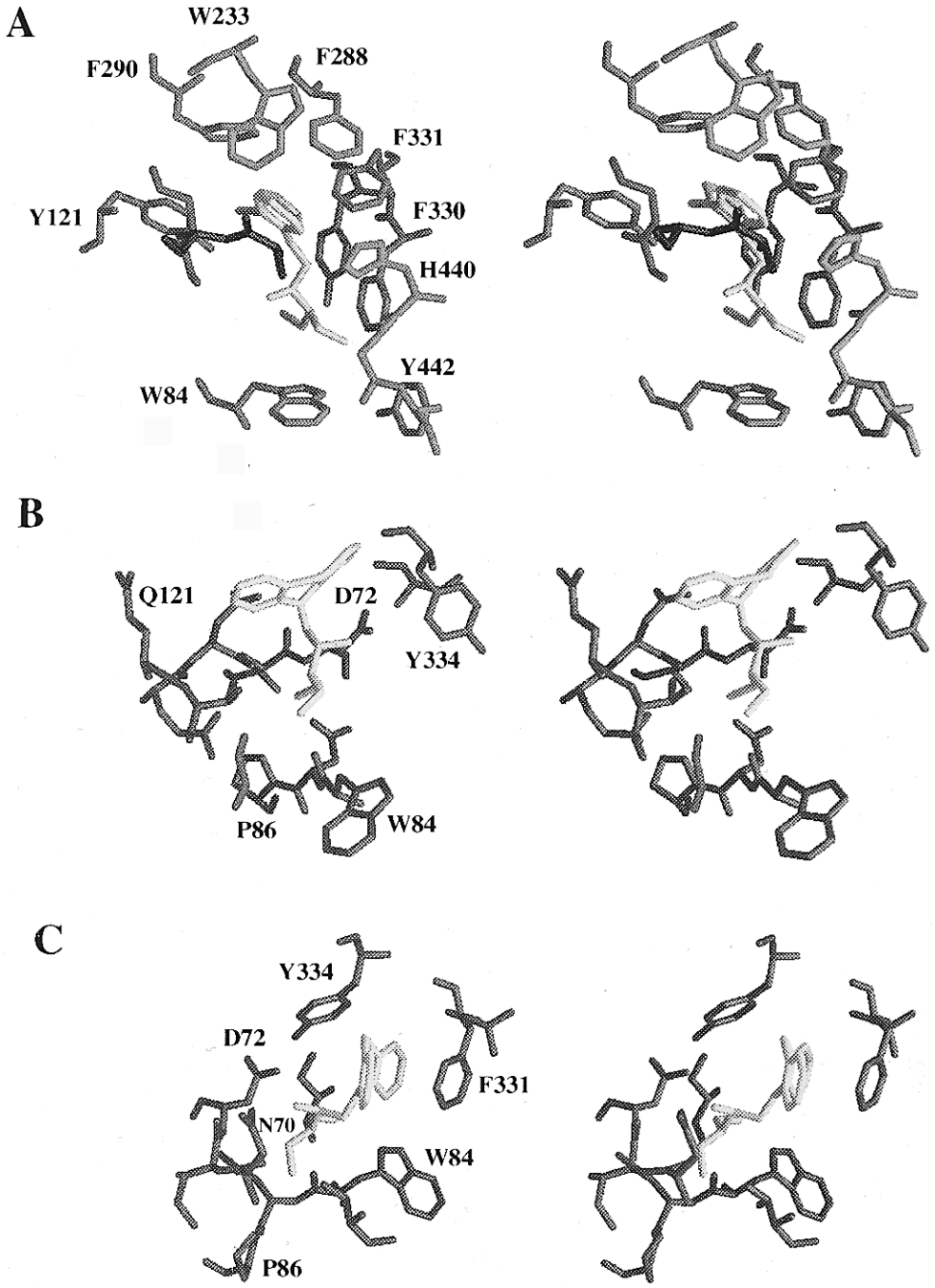

FIGURE 5: Stereoview of ethopropazine modeled into the active site gorge of *Torpedo* AChE and human BChE. (A) The binding of ethopropazine to AChE was modeled using Insight II (version 2.3.0) and the X-ray crystal structures of *T. californica* AChE (*6*) and ethopropazine (*20*). The amino acid residues within 5 Å of the ethopropazine molecule in the active site gorge are shown. The energy-minimized structure of ethopropazine docked into the active site gorge of AChE shows that there are considerable amounts of van der Waals repulsions between the ethopropazine molecule and AChE. G118 and Gl l 9 are shown in cyan and S200 and A201 in blue. (B and C) The atomic structure of human BChE was a reconstructed model based on the structure of *T. californica* AChE (*10*). The energy-minimized structures from the molecular dynamics calculations show that the active site gorge of BChE is large enough to accommodate ethopropazine in two orientations without causing van der Waals repulsion. The figure was generated using GRASP (*42*).

mutation of A328(*F330*) to F (as in *Torpedo* AChE), or Y (as in mammalian AChE), decreases the volume of the active site gorge by ~100 Å^3, but this decrease is not enough to affect the binding of ethopropazine to mutant BChEs (Figure 4G,H). In fact, the energy calculations indicate that the A328(*F330*) mutant of BChE interacts with ethopropazine better than the native protein, probably due to a gained van der Waals interaction. The figure also shows that ethopropazine is accommodated deeper in the active site gorge of AChE compared to BChE.

To evaluate the changes that the enzyme undergoes due to the binding of ethopropazine, we carried out a molecular dynamics simulation. Figure 5 shows ethopropazine modeled into the active site gorge of *Torpedo* AChE (panel A) and human BChE (panels B and C), respectively. The aromatic amino acid residues lining the active site gorge are also shown. The active site gorge in the AChE−ethopropazine complex is very crowded, and the side chains of W84, Y121, W233, F290, and F331 are bent (Figure 5A). These results also show that there are considerable amounts of van

der Waals repulsions between the ethopropazine molecule and AChE (panel A) in two areas: one is between the ethyl group of ethopropazine and F330, W84, and H440 of AChE, which are at a distance of 3.2 Å, and the other is between the tricyclic rings of ethopropazine and Y121 (2.85 Å), F288, F290, and F331 (3.3 Å) of AChE. Besides these interactions there are hydrophobic interactions between the ethyl group of ethopropazine and the side chains of F330 and W84 of AChE and $\pi-\pi$ interactions between the tricyclic rings of ethopropazine and the side chains of Y121, F288, F290, and F331 of AChE.

In contrast, the active site gorge of BChE is large enough to accommodate ethopropazine in two orientations without causing van der Waals repulsion. In both orientations (Figure 5, panels B and C), there is an electrostatic interaction between the side chain of D72 of BChE and the positively charged side chain nitrogen of ethopropazine. In the second orientation (Figure 5C), in addition to the electrostatic interaction, there is a strong $\pi-\pi$ interaction between the side chains of F331 and Y334 of BChE and the tricyclic rings of ethopropazine. The energy difference between the uncomplexed and complexed enzymes in Table 6 shows that both orientations of ethopropazine are equally feasible. These data are in agreement with those of the rigid-body refinement calculations and show that the binding of ethopropazine is less favorable in AChE compared to BChE, making it a poor inhibitor of AChE. The replacement of bulky F330 to A in *Torpedo* AChE increased the size of the gorge, allowing a better accommodation of ethopropazine. This was demonstrated by site-directed mutagenesis studies in which replacement of Y337(*F330*) by A in mouse AChE resulted in enhanced inhibition of mutant enzyme by ethopropazine (*8*). Therefore, both these modeling techniques provide a simple and straightforward explanation for the kinetic data on the specificity of ethopropazine and other bulky inhibitors of ChEs.

DISCUSSION

Substrate Activation. One of the properties that distinguishes BChE from AChE is that the former shows substrate activation with BTC whereas the latter shows substrate inhibition at high concentrations of ATC. Both phenomena are thought to be due to the binding of a substrate molecule at a peripheral anionic site remote from the catalytic site (*7*, *33*). The binding of substrate at the peripheral anionic site allosterically affects the conformation at the active site, thus influencing acylation and/or deacylation rates. It was suggested that substrate inhibition could be affected by changing the conformation of the aromatic residues in the vicinity of the peripheral anionic site (*7*). In this regard it is relevant to mention studies with AChE mutants in which amino acid residues that influenced substrate inhibition were identified. In a study with human AChE mutants, it was shown that the Y337A mutant, and not the Y337F mutant, was resistant to inhibition by excess substrate (*13*). Using molecular modeling studies it was demonstrated that binding of substrate at the peripheral anionic site resulted in a rotation of the side chain of Y337 (A328 in BChE) that could physically block access to the catalytic site (*13*). According to this model, only the aromatic side chain of Y or F and not A was capable of blocking access to the catalytic site, resulting in substrate inhibition. Using site-directed mutagenesis studies, other residues that are also involved in substrate inhibition in AChE were identified as E202(*199*), F297(*290*), F338(*331*), and D74(*72*) (*8*, *13*, *34*). In a recent study it was shown that the D70(*72*)G and W82(*84*)A mutants of human BChE did not display the phenomenon of substrate activation in the presence of excess BTC (*32*). For BChE, three amino acids, A328, D70, and W82, have been implicated in substrate activation.

Binding of Inhibitors to Butyrylcholinesterase. Several recent studies have demonstrated the usefulness of sequence comparisons, X-ray crystallography, molecular modeling, and site-directed mutagenesis experiments in delineating the role of specific amino acid residues in the binding of substrates, inhibitors, and reactivators to ChEs (*7*, *8*, *10*−*13*, *17*, *18*, *32*, *35*−*37*). In most cases there was agreement between the results obtained from molecular modeling, X-ray crystallographic, and mutagenesis studies that were conducted using AChE mutants. In this study we examined the role of A328(*F330*) in the binding of various inhibitors to ChEs using human BChE mutants to determine if the conclusions drawn from studies with AChE mutants could be extended to BChE. For example, in delineating the role of F330 in binding to huperzine A and edrophonium, we found that the results obtained with AChE mutants could be directly correlated with those obtained with native ChEs and site-specific mutants of human BChE. Mutation of Y337(*F330*) to A, as in BChE, reduced the binding affinity of huperzine A by 1000-fold (*17*) and of edrophonium by 20−40-fold (*8*, *11*). Conversely, mutation of residue A328 in human BChE to Y, to test the same position in a BChE background, increased the binding affinities of these inhibitors to values close to that of AChE. These consistent results led to the conclusion that the cation$-\pi$ interactions contributed by the aromatic residue at position 330 play a significant role in the interaction of huperzine A and edrophonium with AChE. These results also suggest that the dimensions of the active site gorge and the presence of other aromatic residues in the gorge had little or no effect on the binding of these two inhibitors to ChEs.

The kinetic data for edrophonium are also supported by the X-ray crystal structure of the *Torpedo* AChE−edrophonium complex, which shows that the aromatic interactions between F330 and the aromatic ring of the ligand make significant contributions to the stabilization of this complex (*16*). However, the recently reported X-ray crystal structure of the *Torpedo* AChE−(−)-huperzine A complex (*38*) shows that the major interaction is a hydrogen bond between the carbonyl group of huperzine A and Y130 of AChE. The cation$-\pi$ interactions between the primary nitrogen group of huperzine A and the aromatic rings of W84 and F330 are minor by comparison. The significance of these minor interactions can be appreciated from our kinetic data which show that the mutation of A328(*F330*) to Y in human BChE increased the binding affinity of (−)-huperzine A to BChE by 6000-fold. Additional evidence for the strength of the interaction of F330 with (−)-huperzine A is the finding that the mutation of Y337(*F330*) to A in mouse AChE reduced the binding affinity 1000-fold (*17*). The presence of an aromatic residue at position 330 is necessary for the binding of huperzine A. Besides Y337(*F330*), there are five other aromatic amino acid residues, Y72(*70*), Y124(*121*), W286(*279*), F295(*288*), and F297(*290*), in the active site gorge of AChE that are replaced by aliphatic residues in BChE. Site-directed mutagenesis studies with human AChE

Table 7: Root Mean Square Difference (in Å) in the C_α Positions of Various Acetylcholinesterase Crystal Structures[a]

	Torpedo AChE	*Torpedo* AChE−tacrine	*Torpedo* AChE−edrophonium	*Torpedo* AChE−decamethonium	*Torpedo* AChE−TMTFA	*Torpedo* AChE−fasciculin
Torpedo AChE−tacrine	0.34					
Torpedo AChE−edrophonium	0.28	0.27				
Torpedo AChE−decamethonium	0.37	0.30	0.27			
Torpedo AChE−TMTFA	0.40	0.31	0.32	0.34		
Torpedo AChE−fasciculin	0.48	0.51	0.48	0.54	0.55	
mouse AChE−fasciculin	0.93	0.90	0.86	0.89	0.90	0.91

[a] The crystal structures were obtained from Brookhaven Protein Data Bank.

mutants W286A, F295A, and F295A/F297V showed that these mutations had only slight-to-moderate effects on the binding of huperzine A (*18*). The importance of cation−π interactions in biological structures is well documented (*39*), and the observed pharmacological data and the molecular model of the AChE−huperzine A complex proposed by Saxena et al. (*17*) support a major role for Y337(*F330*) in the binding and stereoselectivity of (−)-huperzine A for ChEs. Since Y130 is common to all ChEs sequenced to date, it is unlikely that the interaction between huperzine A and Y130 described in the crystal structure can account for the selectivity of huperzine A for AChE.

The discrepancy in the results of kinetic studies and the X-ray crystal structure is not unique to huperzine A and was noted for tacrine also. The X-ray crystal structure of the *Torpedo* AChE−tacrine complex revealed that tacrine was sandwiched between the rings of W84 and F330 (*40*). However, site-directed mutagenesis studies with mouse AChE Y337 and human BChE A328 mutants did not support a role for this residue in the stabilization of the complex observed in the X-ray crystal structure. Our results suggest that tacrine is a more potent inhibitor of BChE because of its favorable accommodation in the larger active site gorge of BChE.

Previous site-directed mutagenesis studies with AChE mutants showed that the cluster of aromatic amino acid residues, Y72(*70*), Y124(*121*), and W286(*279*), located at the lip of the gorge stabilized the binding of substrate and inhibitors like BW284C51, decamethonium, and propidium (*8*, *13*). The significance of the interaction of aromatic groups in BW284C51 with F330 is reflected by a 10−30-fold decrease in K_I observed upon mutation of A328(*330*) to F or Y in human BChE (Table 2). The X-ray crystal structure of the *Torpedo* AChE−decamethonium complex revealed that both quaternary groups were in van der Waals contact with indole rings of W84 and W279, respectively (*40*). Although W286(*279*) is replaced by A in human BChE, consistent with previous observations (*8*), there was no difference in the inhibition of AChE and BChE by decamethonium. These results suggest that the orientation of decamethonium in the larger BChE gorge may be different from that of the AChE gorge. The importance of gorge dimensions in accommodating bulky inhibitors was also seen in the binding of propidium, which is an uncompetitive inhibitor of AChE and a competitive inhibitor of BChE. This is probably because the relatively larger active site gorge of BChE compared to AChE allows the entry and accommodation of propidium and other bulky molecules better than AChE (*8*, *10*, *11*, *32*).

Although the role of A328(*F330*) in the binding of edrophonium, huperzine A, and tacrine to ChEs could be ascertained from site-directed mutagenesis studies with AChE and BChE mutants, this was not the case for ethopropazine. There was a difference in results obtained with mouse AChE Y337 and human BChE A328 mutants, regarding the role of this residue in the binding of ethopropazine to ChEs. Using molecular models of the *Torpedo* AChE−ethopropazine complex and site-specific mutants of mouse AChE, it was demonstrated that Y337(*F330*) sterically occluded the binding of substituted phenothiazines (*8*). Removal of the aromatic side chain produced K_I's resembling those of BChE, suggesting that ethopropazine has a higher affinity for BChE than for AChE because it can be positioned better in the larger active site gorge of BChE. However, substitution of A328(*330*) by aromatic residues such as F or Y did not have any significant effect on the binding of ethopropazine to the mutant BChEs. One possible explanation for this result is that the larger dimension of the BChE active site gorge may allow the positioning of inhibitors in alternate configurations.

Six of the 14 bulky aromatic residues lining the gorge of AChE are replaced by smaller aliphatic residues in BChE. The mutation of residues at positions 295(*288*) and 297(*290*) to aliphatic residues in mouse AChE allowed the entry of bulky substrates and inhibitors into the gorge due to an increase in dimensions of the active site gorge (*38*). However, superimposition of the AChE and BChE active site gorges showed that, besides residues in the acyl pocket, the presence of other aliphatic residues in the gorge increased the dimensions of the BChE gorge. In fact, volume calculations of the active site gorge of ChEs showed that the volume of the BChE gorge was ~200 Å^3 larger than that of the AChE gorge. Rigid-body refinement and molecular dynamics calculations of the ChE−ethopropazine complexes clearly demonstrated that the larger dimension of the BChE gorge allowed the accommodation of ethopropazine in two orientations.

Taken together, these results suggest that although the overall scaffolding of the two enzymes may be highly similar, the dimensions and the microenvironment of the gorge play a significant role in determining the selectivity of substrate and inhibitors for ChEs. Site-directed mutagenesis of an aromatic amino acid residue in the AChE gorge to an aliphatic residue may increase the dimensions of the gorge as in BChE, but the microenvironment of the gorge is essentially that of AChE and not BChE. Therefore, the role of a particular amino acid residue in the binding of an inhibitor should be ascertained by molecular modeling and site-directed mutagenesis studies conducted with both AChE and BChE mutants.

Butyrylcholinesterase Model. Due to the lack of an X-ray crystal structure for BChE, molecular modeling studies with BChE utilized a reconstructed model (*10*). This model of human BChE was developed on the basis of the three-

dimensional structure of *Torpedo* AChE and the 53% sequence identity and 73% sequence similarity between *Torpedo* AChE and human BChE. With this high level of sequence identity and similarity, the estimated C_α rms deviation between the human BChE model and its template X-ray crystal structure of *Torpedo* AChE is expected to be less than 1.0 Å (*41*). Indeed, the modeled human BChE structure closely resembled that of AChE in overall features with the C_α rms deviation between the template X-ray crystal structure of *Torpedo* AChE and the human BChE model being 0.28 Å *(10)*. This value of C_α rms deviation is less than the value of ∼0.9 Å obtained from various crystal structures of *Torpedo* AChE and mouse AChE, which possess 54% sequence identity and 71% sequence homology (Table 7). The human BChE model was used successfully to predict mutations that could impart BChE-like properties to AChE through site-directed mutagenesis studies (*10*). As shown in Table 7, the rms deviation for the C_α atoms of *Torpedo* AChE in the native state and in various complexes ranges from 0.28 to 0.48 Å with an average value of 0.37 Å, suggesting that the enzyme molecule does not undergo significant conformational changes upon complex formation. Although the powerful predictive capability of this model has been demonstrated by site-directed mutagenesis studies, this model will have to be revised when the crystal structure of the BChE molecule is resolved.

ACKNOWLEDGMENT

We thank Naifeng Qian for her contribution to the molecular modeling studies and Dr. Shawn Feaster for discussion and help with the preparation of the figures.

REFERENCES

1. Alles, G. A., and Hawes, P. C. (1940) *J. Biol. Chem. 133*, 375−390.
2. Augustinsson, K. B. (1948) *Acta Physiol. Scand., Suppl. 52*, 1−182.
3. Barnard, E. A. (1974) in *The Peripheral Nervous System* (Hubbard, J. I., Ed.) pp 201−224, Plenum Press, New York.
4. Chatonnet, A., and Lockridge, O. (1989) *Biochem. J. 260*, 625−634.
5. Gentry, M. K., and Doctor, B. P. (1991) in *Cholinesterases: Structure, Function, Mechanism, Genetics and Cell Biology* (Massoulié, J., Bacou, F., Barnard, E. A., Chatonnet, A., Doctor, B. P., and Quinn, D. M., Eds.) pp 394−398, American Chemical Society, Washington, DC.
6. Sussman, J. L., Harel, M., Frolow, F., Oefner, C., Goldman, A., Toker, L., and Silman, I. (1991) *Science 253*, 872−879.
7. Vellom, D. C., Radić, Z., Ying, L., Pickering, N. A., Camp, S., and Taylor, P. (1993) *Biochemistry 32*, 12−17.
8. Radić, Z., Pickering, N., Vellom, D. C., Camp, S., and Taylor, P. (1993) *Biochemistry 32*, 12074−12084.
9. Massoulié, J., Sussman, J. L., Doctor, B. P., Soreq, H., Velan, B., Cygler, M., Rotundo, R., Shafferman, A., Silman, I., and Taylor, P. (1992) in *Multidisciplinary Approaches to Cholinesterase Functions* (Shafferman, A., and Velan, B., Eds.) pp 285−288, Plenum Press, New York.
10. Harel, M., Sussman, J. L., Krejci, E., Bon, S., Chanal, P., Massoulie, J., and Silman, I. (1992) *Proc. Natl. Acad. Sci. U.S.A. 89*, 10827−10831.
11. Ordentlich, A., Barak, D., Kronman, C., Flashner, Y., Leitner, M., Segall, Y., Ariel, N., Cohen, S., Velan, B., and Shafferman, A. (1993) *J. Biol. Chem. 268*, 17083−17095.
12. Fournier, D., Bride, J. M., Hoffman, F., and Karch, F. (1992) *J. Biol. Chem. 267*, 14270−14274.
13. Shafferman, A., Velan, B., Ordentlich, A., Kronman, C., Grosfeld, H., Leitner, M., Flashner, Y., Cohen, S., Barak, D., and Ariel, N. (1992) *EMBO J. 11*, 3561−3568.
14. Kreienkamp, H. J., Weise, C., Raba, R., Aaviksaar, A., and Hucho, F. (1991) *Proc. Natl. Acad. Sci. U.S.A. 88*, 6117−6121.
15. Weise, C., Kreienkamp, H. J., Raba, R., Pedak, A., Aaviksaar, A., and Hucho, F. (1990) *EMBO J. 9*, 3385−3388.
16. Sussman, J. L., Harel, M., and Silman, I. (1992) in *Multidisciplinary Approaches to Cholinesterase Functions* (Shafferman, A., and Velan, B., Eds.) pp 95−108, Plenum Press, New York.
17. Saxena, A., Qian, N., Kovach, I. M., Kozikowski, A. P., Pang, Y.-P., Vellom, D. C., Radić, Z., Quinn, D., Taylor, P., and Doctor, B. P. (1994) *Protein Sci. 3*, 1770−1778.
18. Ashani, Y., Grunwald, J., Kronman, C., Velan, B., and Shafferman, A. (1994) *Mol. Pharmacol. 45*, 555−560.
19. De La Hoz, D., Doctor, B. P., Ralston, J. S., Rush, R. S., and Wolfe, A. D. (1986) *Life Sci. 9*, 195−199.
20. Klein, C. L., Lear, J., O'Rourke, S., Williams, S., and Liang, L. (1994) *J. Pharm. Sci. 83*, 1253−1256.
21. McTiernan, C., Adkins, S., Chatonnet, A., Vaughan, T. A., Bartels, C. F., Kott, M., Rosenberry, T. L., La Du, B. N., and Lockridge, O. (1987) *Proc. Natl. Acad. Sci. U.S.A. 84*, 6682−6686.
22. Chen, B., and Przybyla, A. E. (1994) *Biotechniques 17*, 657−659.
23. Ellman, G. L., Courtney, D., Andres, V., and Featherstone, R. M. (1961) *Biochem. Pharmacol. 1*, 88−95.
24. Levy, D., and Ashani, Y. (1986) *Biochem. Pharmacol. 35*, 1079−1085.
25. Aldridge, W. N., and Reiner, E. (1972) in *Enzyme inhibitors as substrates*, North Holland, Amsterdam.
26. Jones, T. A., Zou, J.-Y., Cowan, S. W., and Kjeldgaad, M. (1991) *Acta Crystallogr. A47*, 110−119.
27. Kleywegt, G. J., and Jones, T. A. (1994) *Acta Crystallogr. D50*, 178−185.
28. Brunger, A. T. (1992) *X-PLOR: A system for X-ray crystallography and NMR*, version 3.1, Yale University, New Haven, CT.
29. Kleywegt, G. J. (1995) in *ESF/CCP4 News Lett. 31*, 45−50.
30. Masson, P., Froment, M.-T., Bartels, C., and Lockridge, O. (1996) *Eur. J. Biochem. 235*, 36−48.
31. Ashani, Y., Peggins, J. O., III, and Doctor, B. P. (1992) *Biochem. Biophys. Res. Commun. 184*, 719−726.
32. Taylor, P., and Lappi, S. (1975) *Biochemistry 14*, 1989−1997.
33. Radić, Z., Reiner, E., and Taylor, P. (1990) *Mol. Pharmacol. 39*, 98−104.
34. Radić, Z., Gibney, G., Kawamoto, S., Bongiorno, C., and Taylor, P. (1992) *Biochemistry 31*, 9760−9767.
35. Masson, P., Legrand, P., Bartels, C. F., Froment, M.-T., Schopfer, L. M., and Lockridge, O. (1997) *Biochemistry 36*, 2266−2277.
36. Hosea, N. A., Berman, H. A., and Taylor, P. (1995) *Biochemistry 34*, 11528−11536.
37. Ashani, Y., Radić, Z., Tsigelny, I., Vellom, D. C., Pickering, N. A., Quinn, D. M., Doctor, B. P., and Taylor, P. (1995) *J. Biol. Chem. 270*, 6370−6380.
38. Raves, M. L., Harel, M., Pang, Y.-P., Silman, I., Kozikowski, A. P., and Sussman, J. L. (1997) *Nat. Struct. Biol. 4*, 57−63.
39. Dougherty, D. A. (1996) *Science 271*, 163−168.
40. Harel, M., Schalk, I., Ehret-Sabatier, L., Bouet, F., Goeldner, M., Hirth, C., Silman, I., and Sussman, J. L. (1993) *Proc. Natl. Acad. Sci. U.S.A. 90*, 9031−9035.
41. Chothia, C., and Lesk, A. M. (1986) *EMBO J. 5*, 823−826.
42. Nicholls, A., Sharp, K. A., and Honig, B. (1991) *Proteins 11*, 281−296.

BI971425+